Microglia influence host defense, disease, and repair following murine coronavirus infection of the CNS

Amber R. Syage, Vrushali Mangale, H. Ataken Ekiz, Dominic D. Skinner, Yuting Cheng, Colleen Stone, Ryan M. O'Connell, Kim N. Green, and Thomas E. Lane

Department of Pathology, Division of Microbiology & Immunology, University of Utah, School of Medicine, Salt Lake City, Utah 84112

Introduction

Background:

- Mice infected with the neurotropic JHM strain of mouse hepatitis virus (JHMV) suffer from acute encephalomyelitis and chronic demyelination within the central nervous system (CNS).
- Immunologic control of viral replication within the CNS is complex, involving both the innate and adaptive immune response.
- Neuropathology is mediated by local glial responses working in combination with components of the innate and adaptive responses.

Goal: To understand the functional contributions of microglia in host defense and demyelination in response to JHMV infection of the CNS

Approach:

- Treated mice with PLX5622, an inhibitor of colony stimulating factor 1 receptor (CSF1R), that efficiently depletes microglia.
- Conducted single cell RNA sequencing (scRNASeq) on CD45+ cells isolated from the CNS of PLX5622 and control-treated mice at days 7 and 14 p.i.
- Evaluated spinal cord demyelination at day 14 and 21 p.i. and remyelination at day 21 p.i.

Methods/Results

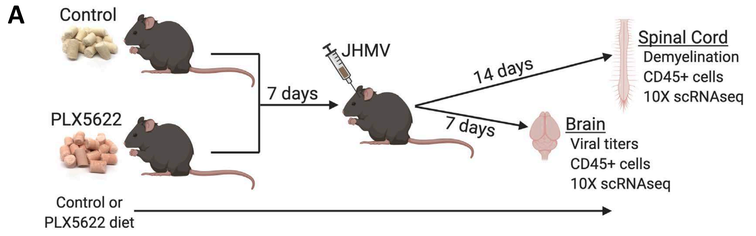

PLX5622 Treatment:

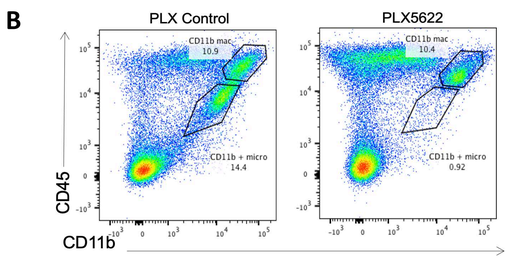

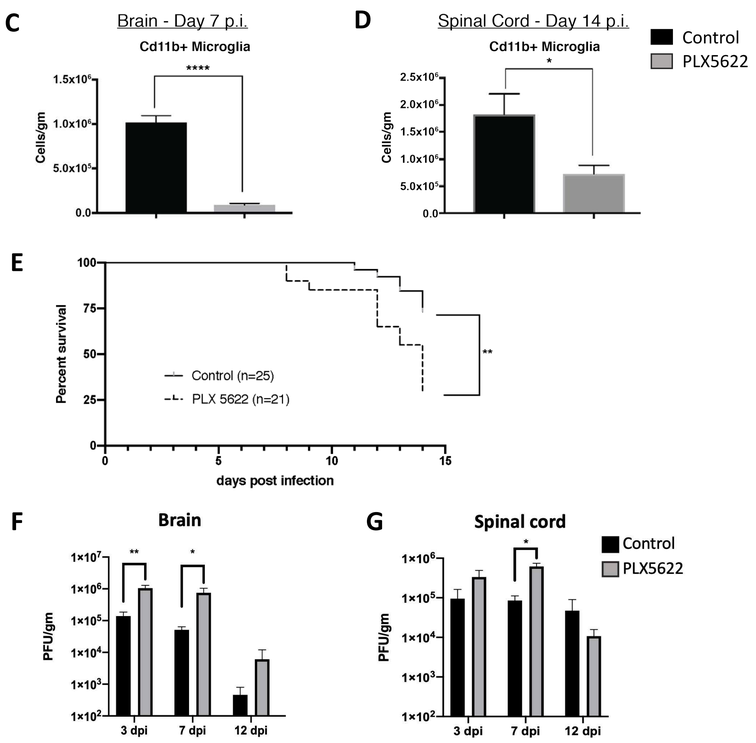

Figure 1: (**A**) Schema of experimental design. (**B**) Representative flow cytometry data from JHMV-infected mice treated with either PLX5622 or control chow and gating on microglia cells ($CD45^{lo}CD11b^{+}$ cells). Quantification of flow cytometric data shows a reduction of microglia in PLX5622-treated mice vs. controls from brains at day 7 p.i. (**C**) and spinal cords at day 14 p.i. (**D**). (**E**) Survival curve reveals higher mortality in PLX5622-treated mice. Viral titers measured from brains at days 3, 7, and 12 p.i. display reduced viral clearance in PLX5622-treated mice in both brains (**F**) and spinal cords (**G**). *p≤ 0.05; ** p≤ 0.01; ****p≤ 0.0001.

Day 7 post-infection - Brain

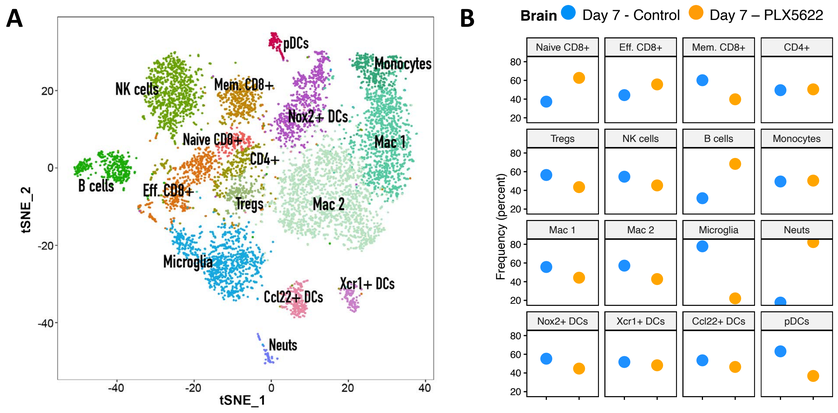

Figure 2: (**A**) Unsupervised clustering analysis of cells from brains at day 7 p.i. following scRNAseq. **(B)** DotPlot representing percentage of cells from control (blue) versus PLX5622 (orange) within a cluster (pooled brains from 5-6 mice/experimental group).

Depletion of microglia dampens macrophage APC activity and CD4⁺ T cell responses

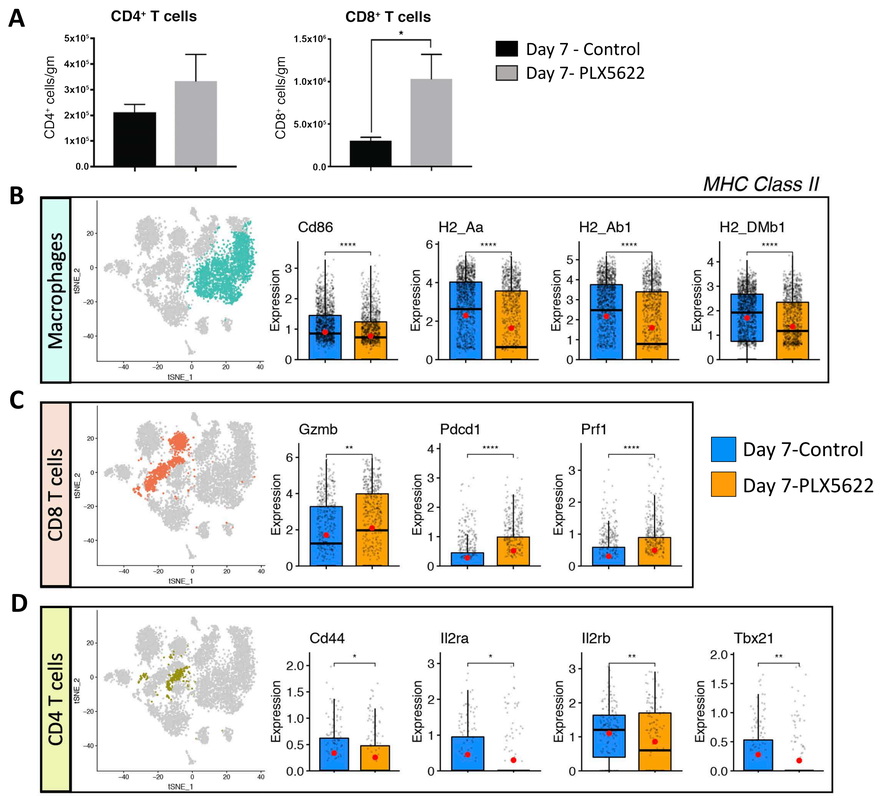

Figure 3: Brains of control (black, blue) and PLX5622-treated (grey, orange) mice at 7 d.p.i. (**A**) Quantification of flow cytometric data of infiltrating CD4 and CD8 T cells (n=6/group). Box plots comparing expression of activation markers *Cd44* , *Il2ra, Il2rb,* and *Tbx21* (T-bet) in CD4 T cells (**B**), effector markers *Prf1* (Perforin), *Pdcd1* (Programmed cell death 1), and *Gzmb* in CD8 T cells (**C**), and MHC class II genes and co-stimulatory molecule *Cd86* in macrophages (**D**). Plots show interquartile range, median value (bold horizontal bar) and average expression per sample (red dot). Used Wilcoxon test, *p≤ 0.05; ** p≤ 0.01; ****p≤ 0.0001.

Day 14 and Day 21 post-infection – Spinal Cord

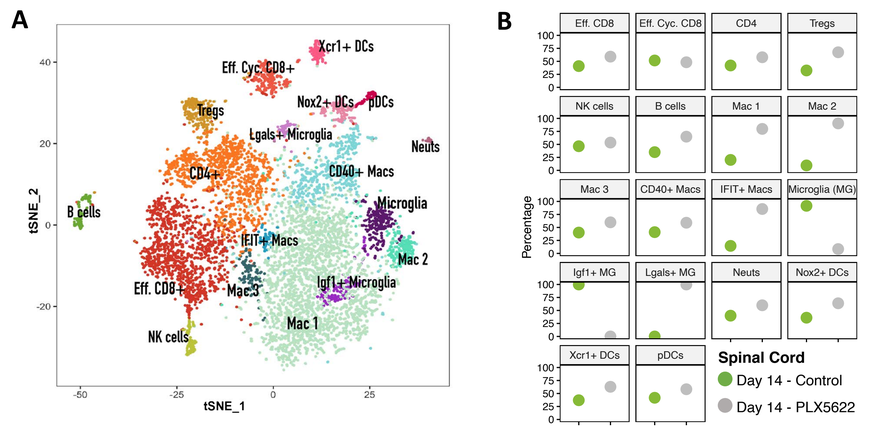

Figure 4: (**A**) Unsupervised clustering analysis of cells from spinal cords at 14 d.p.i. after scRNAseq. (**B**) DotPlot representing percentage of cells from control (green) and PLX5622-treated (grey) mice within a cluster (pooled spinal cords from 6-7 mice/experimental group).

Microglia depletion increases demyelination

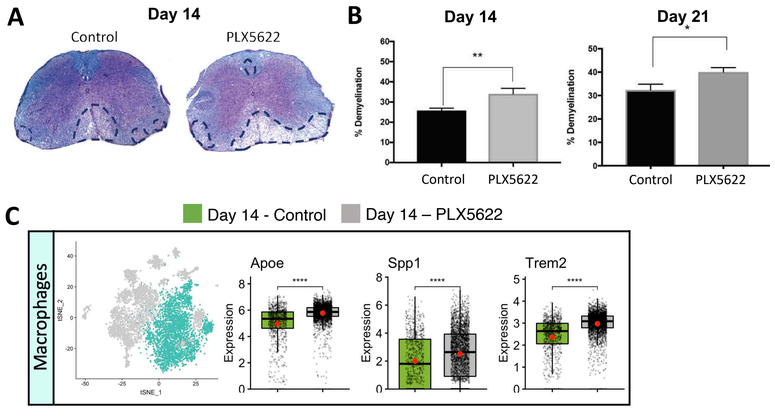

Figure 6: (**A**) Representative images of H&E/LFB-stained spinal cord sections showing increased demyelination (dashed lines) in JHMV-infected mice treated with PLX5622 vs controls at 14 d.p.i. (**B**) Quantification of demyelination reveals a significant increase in PLX5622-treated mice at days 14 and 21 p.i. (min. of 12 mice/group). (**C**) Expression of *Apoe, Spp1(Osteopontin),* and *Trem2* in spinal cords of PLX5622-treated (green) versus controls (grey) in all macrophages at 14 d.p.i. *p≤ 0.05; **p≤ 0.01; ****p≤ 0.0001.

Microglial depletion reduces capacity to remyelinate

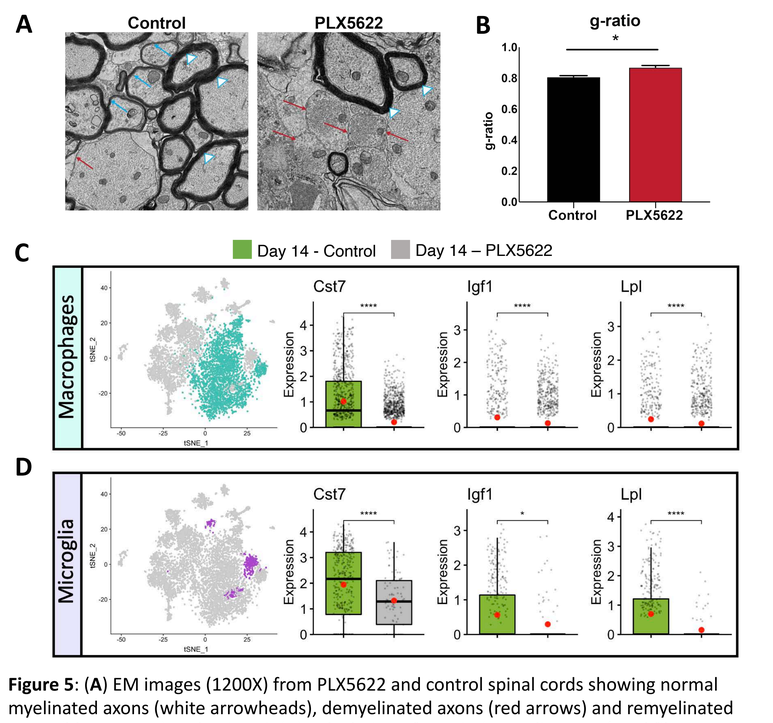

Figure 5: (**A**) EM images (1200X) from PLX5622 and control spinal cords showing normal myelinated axons (white arrowheads), demyelinated axons (red arrows) and remyelinated axons (blue arrows) at day 21 p.i. (**B**) Calculation of g-ratio (axon diameter/total fiber diameter) of PLX5622 and control. Box plots comparing expression of transcripts of remyelination-associated markers *Cst7* (Cystatin F), *Igf1* (Insulin-like growth factor 1), and *Lpl* (Lipoprotein lipase) in merged microglia (**C**) and macrophage (**D**) populations in spinal cords of control (green) and PLX5622-treated (grey) mice. *p≤ 0.05; ****p≤ 0.0001.

Perspectives

Day 7 p.i. – Brains

- Microglia aid in control of viral replication
- Depletion of microglia results in an inability to prime a Th1 response in $CD4^{+}$ T cells

Day 14 and 21 p.i. – Spinal Cords

- Microglia potentially play a protective role by restricting white matter pathology and contributing to remyelination

Acknowledgements

This work was funded by the National Institutes of Health (NIH) R01NS092042, NIH R01NS99255, and the Ray and Tye Noorda Foundation.